THIS IS A PEER REVIEWED PAPER
FIG Working Week 2012

GNSS antenna offset field test in Metsähovi

Ulla KALLIO, Hannu KOIVULA, Sonja NYBERG, Pasi Häkli, Paavo Rouhiainen, Veikko Saaranen, Finland
Zane Cirule, Didzis Dobelis, Vladimirs Golovka, Latvia

Key words: GNSS antenna offset, field calibration

SUMMARY

The phase center variation and the mean phase center of the GNSS antenna can be determined in the robot calibration. We have studied how well the offset values are valid in the field and the consistency between two sets of antennas of different type.

We measured 24 full 48-hour-sessions in our relative GNSS antenna field calibration test at Metsähovi fundamental station during three months in summer 2011. We chose the full roving observation strategy (Banyai 2005) and circulated nine Ashtech Choke Ring antennas without radome and eight Leica AR25 antennas with radome on three concrete pillars. Data were processed with Bernese GPS Software ver. 5.0 and offset estimation was coded using Octave software. In the Bernese processing we used the Geo++ absolute calibration offset values but in combining the 24 session solutions we still found significant antenna dependent offsets especially in L2 solution between the two antenna types.

The offset values of the individual absolute calibration were not consistent between the two antenna types tested in Metsähovi. There seems to be biases which propagate to the coordinate results. Changing the antenna type in a permanent station may cause cm level jump in time series due to the errors in the offset values even if the individual absolute calibration tables are applied in data processing.

GNSS antenna offset field test in Metsähovi

Ulla KALLIO, Hannu KOIVULA, Sonja NYBERG, Pasi Häkli, Paavo Rouhiainen, Veikko Saaranen, Finland
Zane Cirule, Didzis Dobelis, Vladimirs Golovka, Latvia

ABSTRACT

The phase center variation and the mean phase center of the GNSS antenna can be determined in the robot calibration. We have studied how well the offset values are valid in the field and the consistency between two sets of antennas of different type.

We measured 24 full 48-hour-sessions in our relative GNSS antenna field calibration test at Metsähovi fundamental station during three months in summer 2011. We chose the full roving observation strategy (Banyai 2005) and circulated nine Ashtech Choke Ring antennas without radome and eight Leica AR25 antennas with radome on three concrete pillars. Data were processed with Bernese GPS Software ver. 5.0 and offset estimation was coded using Octave software. In the Bernese processing we used the Geo++ absolute calibration offset values but in combining the 24 session solutions we still found significant antenna dependent offsets especially in L2 solution between the two antenna types.

The offset values of the individual absolute calibration were not consistent between the two antenna types tested in Metsähovi. There seems to be biases which propagate to the coordinate results. Changing the antenna type in a permanent station may cause cm level jump in time series due to the errors in the offset values even if the individual absolute calibration tables are applied in data processing.

1. INTRODUCTION

In many engineering and scientific applications the accuracy of the Global Positioning System (GPS) is often pushed beyond the limits stated by the manufacturers. GPS has proven to be an excellent tool for e.g. monitoring the deformation of bridges or dams, and also crustal deformations. The benefit compared with traditional methods is that inter-station visibility is not needed and accuracy seems to be superior to the traditional methods especially when the measurement area is large. Common for all these applications are that even a millimeter precision with respect to a reference point may be achieved. When monitored periodically or continuously the precision of change detection may reach sub-millimeter accuracy if time series are long enough, typically several years.

The error budget of GPS is generally well known. Some uncertainties come from effects of the ionosphere and troposphere for signal propagation. Major limitations today are the near-field and antenna related effects. Most of the GPS pre-processing software include a calibration values for at least the antennas produced by their own vendors. These values are the same for all the antennas of same type and it is assumed that the differences within

antenna type are not existing or insignificant.

We have noticed a difference between the length of GPS and EDM baseline observed over a same pair of concrete pillars (Kallio et. al., 2009). We considered EDM measurements to be correct since the baseline was measured with a calibrated Kern Mekometer ME5000 with a traceability chain to the definition of meter. One reason for the difference could be non-calibrated GPS antennas. GPS antennas may be calibrated with respect to a reference antenna over a short baseline (Mader, 1999) or in anechoic chamber or using a calibration robot that tilts and rotates the antenna during calibration (Wübbena et al., 2000). Görres et al. (2006) showed that anechoic chamber and robot calibration results agree in mm-level when identical antennas are compared. We chose to use robot calibration and sent our antennas for individual calibration to Geo++. After the calibration, we studied the effect of antenna calibrations on metrologically accurate baselines (Koivula et. al., 2011). Even after the calibration some discrepancies between EDM and GPS remain on the individual antenna level.

There are several possibilities for investigating and evaluating the calibration results. The simplest way is to use a known baseline as a ground truth. More advanced way is to use a reference antenna and use the antenna rotation method. This way the North and East offsets may be determined, but for the Up component a ground truth is necessary. By using an antenna swap method all North, East and Up offsets may be evaluated with respect to the reference antenna. The permutation method, full roving stategy (in Bányai, 2005) lets us evaluate the North, East and Up offsets with respect to chosen antenna or relative to the mean of the antennas used in the test.

The antenna calibration by Geo++ eliminates mostly the effect of the multipath in the calibration values. In the real measurement environment the near-field effects and multipath effect are one of the main error sources in GPS solutions. Antenna calibration values include the effect of the antenna mounting during the calibration. We do not precisely know how much the near field effect changes when we set up the antennas in the field. Zeimetz and Kuhlmann (2011) have tested the near field effect using two different types of mountings showing that different antenna mounting may lead to differences of several millimeters in GPS solution. The ideal case would be a possibility to calibrate or at least test the antennas in the final near-field condition. Normally it is not possible and the best choice is to use the same pillar types and mountings in the test as at the station antenna will be installed.

In this paper we show results from the permutation method that allows us to see the residual North, East and Up antenna offsets for seven Ashtech choke ring and eight Leica choke ring antennas.

2. MEASUREMENTS AT METSÄHOVI

In order to get antennas pointed to the North we marked the true North to the pillar points with tachymeter using the calculated azimuths between the pillars. The observation strategy was tested making some simulations. In simulations we had up to five pillar points. Among the eight nearby pillars in Metsähovi we chose the three pillars which were closest to each

other; the distances between pillars were only 5–13m (Fig 1 and 2). The visibility to the satellites was ensured by cutting the nearest bushes and trees.

We started the test measurements July 13, and ended them October 2, 2011. The antennas were circulated on the three concrete pillars (Fig. 1 and 2). The antenna platform is made of stainless steel with a 5/8 inch hole in the middle to use a standard-sized bolt for the antenna.

The pillar types and antenna platforms we used in the test were similar than in the stations the antennas will be in future. An antenna is directly attached to the platform without any interface or forced centering device, hence its height and position is preserved. No rotations of antennas between sessions were needed thus all antennas were always directed to the North. Each antenna participated at least in three full 48-hours-sessions. Between the sessions antennas were moved to the next pillar. After three sessions two antennas were changed. Altogether 24 sessions were measured. The permuting strategy is shown in the Fig 2. The Ashtech Choke Ring (ASH700936C_M) antenna (sn. 11988) was used as a reference and it participated all the 24 sessions during the three months period. The cut off angle during measurements was 5 degrees.

Figure 1. Zane Cirule, Didzis Dobelis and Vladimirs Golovka made the field work of the antenna test.

3. COMPUTATION WITH BERNESE

The coordinate solutions were computed using Bernese GPS software version 5.0 (Dach et al., 2007). The data processing strategy was based on the double-difference approach. We computed separately L1 and L2 solutions with Geo++ individual absolute calibration tables using the offsets in tables and with zero phase center offsets using only phase center variations.

We used the IGS rapid orbits and earth orientation parameters, because they were available soon after the measurements and are still nearly as accurate as the final products. The observables were screened before ambiguity resolution. A few sessions with lower data quality was detected. Ambiguites were solved using the sigma strategy (Dach et al., 2007). Local ionosphere models were created using the Bernese software. The troposphere was modelled using Saastamoinen apriori model mapped with Dry Niell mapping function. Zenith path delay paremeteres were estimated using Wet Niell mapping function at 2-hour intervals. The observation cut-off angle was set to 10 degrees.

	440	504	505
1	988	22	40
2	40	988	22
3	22	40	988
4	988	3	5
5	5	988	3
6	3	5	988
7	988	6	7
8	7	988	6
9	6	7	988
10	988	11	12
11	12	988	11
12	11	12	988
13	988	194	754
14	754	988	194
15	194	754	988
16	988	761	770
17	770	988	761
18	761	770	988
19	988	772	959
20	959	988	772
21	772	959	988
22	988	963	995
23	995	988	963
24	963	995	988

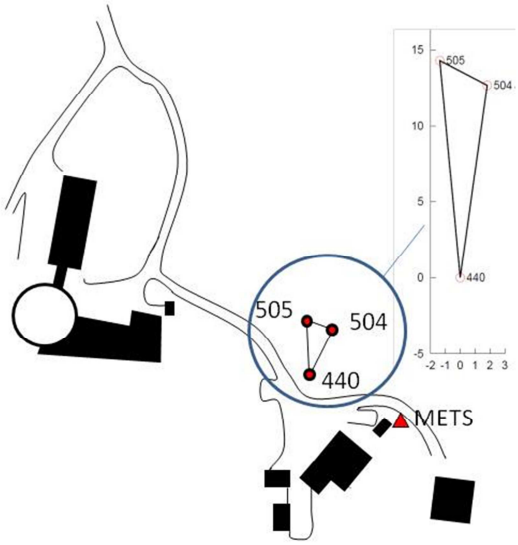

Figure 2. The network (points 440, 504 and 505) in our antenna test in Metsähovi and observation strategy, antenna set up (serial no.) in the sessions 1-24.

The datum was defined by constraining one of the pillar points (440) to its ITRF2008 coordinates in the mid-epoch of the measurement campaing. As a result we achieved four SINEX files for each session (i.e. two solutions for both frequencies with offset values from calibration tables and zero phase center offsets).

4. ESTIMATION OF OFFSETS

Antenna offset calculation precedure was the following: reading the coordinates and covariance matrices from the SINEX file of the session; calculating the coordinate differences (eq. 1) and the covariance matrix, and further the weight matrix (eq. 4 and eq. 5); updating the normal equations (eq. 6); solving the normal equations (eq. 7) and calculating some test statistics (eq. 10). This process was repeated separately for L1 and L2 solution.

In the ideal case, after applying the individual antenna calibration values in the Bernese processing, the estimated offsets are zeros because calibration values should take into account differences between the individual antennas. Including the phase models we can call the estimated offset parameters as residual antenna offsets.

4.1 Mathematical model

To solve for the offset values (*O*) we used the coordinate differences (*dX*) between pillars as pseudo observations in the least squares adjustment. The unknown parameters in the adjustment were the station coordinates and antenna offset values. The direction of the offset

vector depends on the direction of the antenna orientation at a point (plumb line, how well the antenna is levelled on the platform). Because our points were so close to each other we neglected the rotation of the offset vector from the equations and parameterised offset vectors in the global orientation. If the full roving strategy is used in larger area the rotation of offset vectors must be included to the model, as presented in (Bányai 2005). The model is a simple linear differencing. With *n* points, 3(*n*-1) linearly independent equations can be formed

$$dX = D \cdot X_B = D \cdot (X + O_i). \tag{1}$$

Here X_B includes the coordinate solution vector of one session and O_i is the permutation of antennas in the session. D is a differencing operator. In our case with three points we had six observations in each session: the vectors from 440 to 504 and to 505:

$$D = \begin{pmatrix} -1 & 1 & 0 \\ -1 & 0 & 1 \end{pmatrix} \otimes \begin{pmatrix} 1 & 0 & 0 \\ 0 & 1 & 0 \\ 0 & 0 & 1 \end{pmatrix},$$

$$X = \begin{pmatrix} X_{440} \\ X_{504} \\ X_{505} \end{pmatrix}, \tag{2}$$

$$O_1 = \begin{pmatrix} O_{ref} \\ O_a \\ O_b \end{pmatrix}, O_2 = \begin{pmatrix} O_b \\ O_{ref} \\ O_a \end{pmatrix}, O_3 \begin{pmatrix} O_a \\ O_b \\ O_{ref} \end{pmatrix}$$

O_1 O_2 and O_3 include the offset unknowns in three sessions. O_{ref} is 3x1 offset vector for the reference antenna. O_a and O_b are the offset vectors for the other two antennas. Circulation of the antennas on three pillars can be seen as a changing of the order of the offset vectors in equations. The design matrix (A) in the adjustment for the first session is

$$A_1 = (D \quad | \quad D \quad 0 \quad \cdots \quad 0) \tag{3}$$

In the subsequent sessions the first part of the matrix A (station coordinate part) is similar to the first session but the second part (offset parameter part) is a permutation of its columns.
The weight matrix W_{dX} in the adjustment is the inverse of the covariance matrix of coordinate differences. The full covariance matrix (C_x) of coordinates from the Bernese session solution is used. According to the error propagation law the covariance matrix of coordinate differences is:

$$C_{dX} = DC_xD^T \tag{4}$$

$$W_{dX} = (DC_xD^T)^{-1}. \tag{5}$$

The normal equation matrix and the vector are

$$N = \sum A_i^T W_{dx_i} A_i$$
$$t = \sum A_i^T W_{dx_i} dX_i \quad (6)$$

The normal equation matrix is singular and we cannot find a solution by inverting it. Using the Moore-Penrose pseudo inverse we get the station coordinates relative to the center of the network and the antenna offsets relative to the mean of the offsets:

$$\binom{X}{O} = N^+ \cdot t. \quad (7)$$

The rank deficiency of N is six; the translations of the network of the points and the network of antenna offset vectors are undetermined. (When considering the offset unknown part of the design matrix A we can see that the offset vectors form logically a network). Easier way to remove the deficiency is to fix station coordinates of one point and the antenna offset values of one reference antenna, after which we will get offset values relative to the chosen reference antenna. Before comparing the offset vectors or differences of the offset vectors with Geo++ calibration we converted them to the local (North, East, Up) system.

5. ANALYSING THE RESULTS

5.1 Explaining the variation in station coordinates

First we studied the variation of the station coordinates between the 48-hour-sessions. The variation of the station coordinates seems to be as it is in usual GPS time series (Fig. 3 and 4). The session results are dependent on individual antennas even if the individual absolute calibration values of antennas are applied in Bernese processing. This can be seen especially in L2 solution (Fig. 3, Fig. 4 and Fig.5). We can improve the results by determining additional antenna specific residual offset parameters. In Figure 3 and 4 we show how well the variation of station coordinates can be explained with the antenna change. The maximum minus minimum for North, East and Up coordinate residuals before applying the residual offset parameters (just combining the session solutions) were in L1 solution 0.6, 0.9 and 3.5mm, respectively. After estimating the residual offset parameters they were 0.4, 0.8 and 2.5 mm. The improvement in L2 solution was more outstanding: from 1.1, 1.2, and 7.5 mm to 0.8, 1.1 and 3.7 mm between minimum and maximum residuals.

5.2 Comparing the GPS height difference with “ground truth”

Besides the offset calculations we compared the levelled height difference between two pillar points (440 and 504) with GPS results. We computed the ellipsoidal height differences from coordinates after Bernese processing for each session. We computed also the differences of estimated residual offset values between the pillars for every session and found out that they fit well to the levelled minus GPS height difference. The correlation between offset differences and the levelled-GPS height is 66.8% in L1 and 94.6% in L2 with session 16 and

without the session 16 they were 80.1% and 97.8, respectively. This is the part of the variation in the height difference we can explain by the antenna change. As we can see in Fig. 3 and 4 the residuals in session 16 don't belong to the same distribution than other residuals and we may expect that the coordinates of session 16 are outliers. Therefore we removed the session and two subsequent sessions (including the same antennas) from further analysis. To complete our antenna test we will repeat the measurements with antennas participated in sessions 16-18 in the near future.

If we remove the estimated residual antenna offsets our session height differences agree with levelled height difference in the mm-level also in L2 solution (Fig 5). After that the GPS minus levelled height difference should indicate the geoid undulation difference between the pillars. We can still see a small disagreement between the sessions where the Leica and Ashtech antennas have been present.

The residual offsets for all remaining 15 antennas are presented in Fig 6 and 7. Figures 3 and 4 show the size of jumps we can have in our data series although we have used absolute calibration tables in data processing.

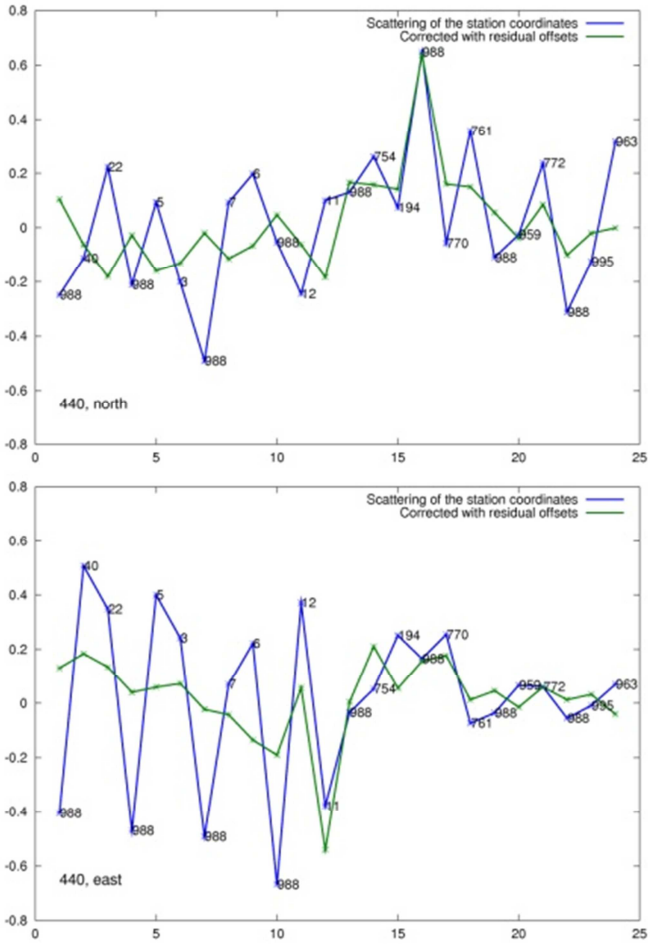

Figure 3. The variation of station coordinates in L2 solution (North and East) before (blue) and after (green) removing the residual offsets in pillar 440 in mm. Antenna number of each session is included in figure. Values are in mm.

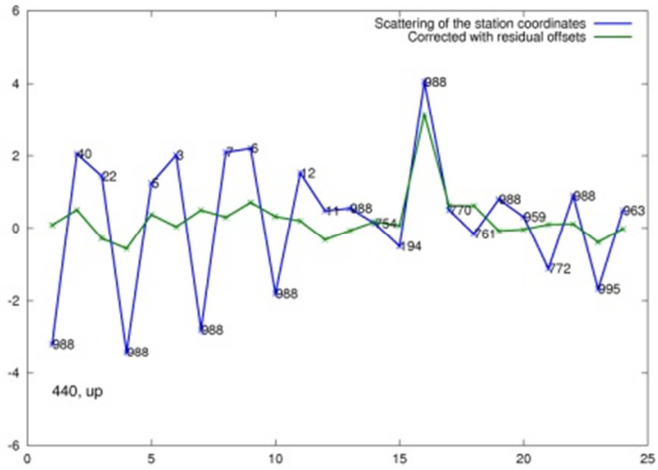

Figure 4. The variation of station coordinates in L2 solution (Up) before (blue) and after (green) removing the residual offsets in pillar 440 in mm. Antenna number of each session is included in figure. Values are in mm.

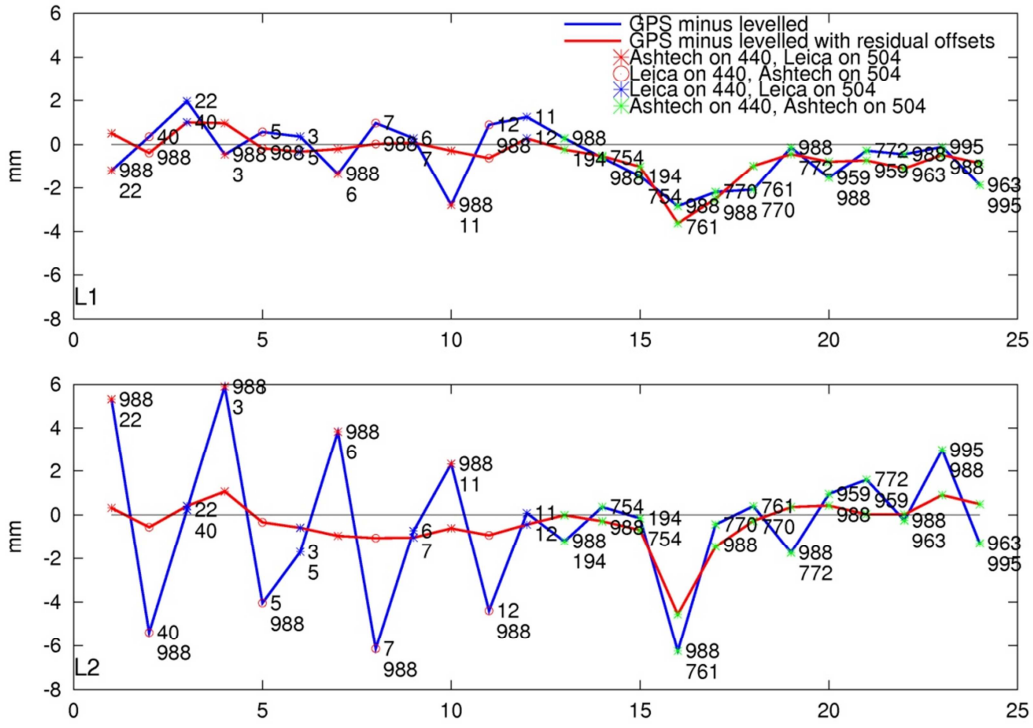

Figure 5. GPS minus levelled height differences with and without the residual antenna offset correction in L1 and in L2 solution. The antenna serial numbers in pillars 440 and 504 are printed in each session.

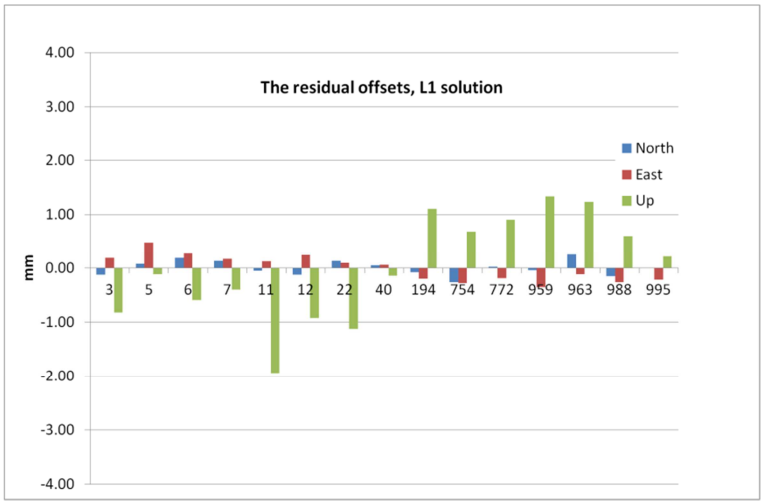

Figure 6. The residual offsets of 15 antennas in L1 (solutions: North (blue), East (red) and Up (green) components for each antenna. The first eight antennas are Leicas and the last seven Ashtechs. Sessions 16-18 were removed from solutions

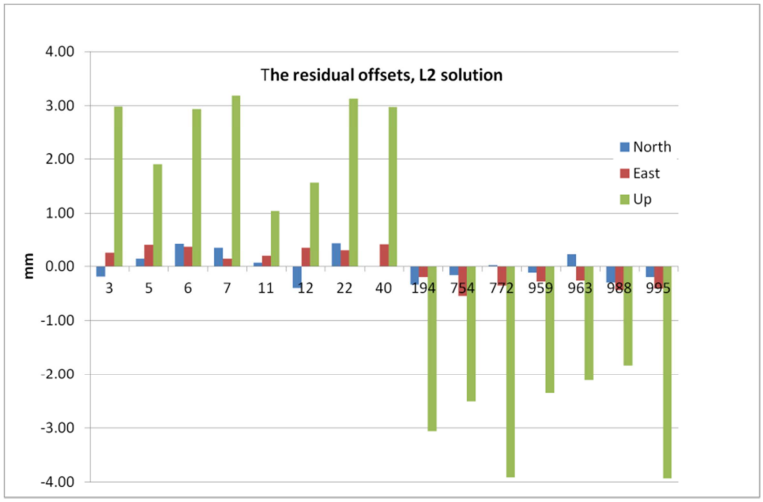

Figure 7. The residual offsets of 15 antennas in L2 solutions: North (blue), East (red) and Up (green) components for each antenna. The first eight antennas are Leicas and the last seven Ashtechs. Sessions 16-18 were removed from solutions.

5.3 Testing the offset parameters

After an adjustment of offset parameters we made the Chi-squared test for the variance factor. As we expected it differs significantly from 1. After removing sessions 16-18 we decided to use the estimated variance factor when calculating the covariance matrix of parameters.
When analysing the results of the computations where the offset values were from the Geo++ calibration values we can test the hypothesis that the calculated offset values are zeros

$$H_0: O = 0$$
$$H_1: O \neq 0 \quad (8)$$

The O in our case is (45x1)-vector and the 0 is a zero vector of the same size. The degree of freedom, r, in the adjustment where the number of sessions is s, the number of points is p and the number of antennas is a is:

$$r = 6 \cdot s + 6 - 3 \cdot p - 3 \cdot a \quad (9)$$

In our case r is 78. We can use the F-distributed test statistic for testing all the offset parameters at the same time:

$$\frac{(O-0)^T C_o^{-1} (O-0)}{u_o} \sim F_{u_o,r} \quad (10)$$

where u_o is the number of offset parameters to be tested (in our case 45). C_O is the part of the estimated covariance matrix of unknowns

$$C_{\hat{x}} = \hat{\sigma}_0^2 N^+ \quad (11)$$

that includes the variances and covariances of the offset parameters. The variance factor has been estimated. The null hypothesis will be rejected if

$$F_{o,r} > F(\alpha, u_o, r). \quad (12)$$

We made the same test for North, East and Up components of the residual offsets separately. Before the test the covariance matrix C_O of the offset parameters were converted to the covariance matrix of the North, East and Up components. To find out the significantly differing antennas we studied offset parameters also component by component, and calculated the 95% confidence intervals for each North, East and Up component.

The estimated residual antenna offsets relative to the mean of all offsets are presented in Table 1. The statistically significant offset components are bolded. The significance depends on the chosen reference. The test statistics and table values of F-distribution are presented in Table 2 for L1 and L2 solutions. When testing all offset parameters together the test statistics indicates that the estimated offset parameters differ significantly from zero and the zero hypothesis should be rejected.

When we test separately Ashtech or Leica antennas we don't get so many statistically significant residual offsets. The test statistics for Leicas and Ashtechs separately are presented in Table 2. We can still argue that between the two antenna types or perhaps the radome types (with and without) there is a significant residual offset especially in L2. This is a signal of systematic errors in the absolute calibration values.

In table 2 the test statistics in the first three rows show if the residual offsets differ from the zero with respect to the mean of the residual offsets. In the first row all components are tested together and then in the next two rows horizontal and vertical components separately. The test

shows that the individual absolute calibration values are biased and if we use all 15 antennas in the same campaign some systematic errors will remain in the results due to insufficient handling of the antenna offsets. The next three rows tell us how well the absolute calibration values fit if only seven Ashtech antennas (the two antennas in sessions 16-18 were not included in the test) are used together and the last three rows the same for eight Leica antennas (i.e. if the different antenna types are not mixed together). There are no significant residual offsets if only Leicas are concerned and there is only some small significant residual offsets in L2 for Ashtech antennas.

Table 1. Estimated residual antenna offsets relative to the mean in L1 and in L2 in mm.

L1	Offsets								
Antenna	North	East	Up	Std /North	Std/ East	Std/ Up	95%/North	95%/East	95%/Up
3	-0.12	0.19	-0.82	0.17	0.11	0.52	0.34	0.23	1.04
5	0.08	**0.48**	-0.12	0.17	0.11	0.52	0.34	0.23	1.04
6	0.18	**0.27**	-0.59	0.19	0.13	0.57	0.37	0.25	1.14
7	0.13	0.17	-0.40	0.19	0.13	0.57	0.37	0.25	1.14
11	-0.05	0.12	**-1.94**	0.22	0.14	0.65	0.43	0.29	1.30
12	-0.13	0.24	-0.93	0.22	0.14	0.66	0.43	0.29	1.31
22	0.13	0.10	-1.13	0.19	0.13	0.58	0.38	0.26	1.16
40	0.05	0.06	-0.14	0.19	0.13	0.59	0.38	0.26	1.17
194	-0.08	-0.20	**1.10**	0.17	0.12	0.54	0.35	0.23	1.07
754	-0.26	**-0.28**	0.68	0.18	0.12	0.55	0.35	0.23	1.09
772	0.02	-0.19	0.90	0.17	0.11	0.52	0.34	0.22	1.03
959	-0.04	**-0.36**	**1.33**	0.17	0.11	0.52	0.34	0.22	1.03
963	0.25	-0.11	1.23	0.15	0.10	0.47	0.30	0.20	0.94
988	-0.15	**-0.26**	**0.60**	0.06	0.04	0.18	0.12	0.08	0.36
995	0.00	**-0.22**	0.22	0.15	0.10	0.47	0.31	0.20	0.94
L2	Offsets								
Antenna	North	East	Up	Std /North	Std/ East	Std/ Up	95%/North	95%/East	95%/Up
3	-0.19	**0.25**	**2.98**	0.17	0.11	0.52	0.34	0.23	1.04
5	0.14	**0.42**	**1.90**	0.17	0.11	0.53	0.34	0.23	1.05
6	**0.43**	**0.38**	**2.94**	0.19	0.13	0.59	0.39	0.26	1.18
7	0.36	0.14	**3.19**	0.19	0.13	0.59	0.38	0.26	1.17
11	0.07	0.20	1.04	0.24	0.16	0.74	0.48	0.32	1.46
12	-0.40	**0.36**	**1.56**	0.24	0.16	0.74	0.48	0.32	1.48
22	**0.45**	0.31	**3.13**	0.20	0.14	0.62	0.41	0.27	1.23
40	0.00	**0.43**	**2.98**	0.21	0.14	0.63	0.41	0.27	1.25
194	-0.34	-0.20	**-3.06**	0.19	0.13	0.60	0.39	0.26	1.20
754	-0.16	**-0.55**	**-2.51**	0.20	0.13	0.61	0.39	0.26	1.22
772	0.03	**-0.35**	**-3.91**	0.19	0.13	0.59	0.38	0.25	1.17
959	-0.12	**-0.28**	**-2.36**	0.19	0.13	0.58	0.38	0.25	1.16
963	0.23	**-0.26**	**-2.12**	0.17	0.11	0.52	0.33	0.22	1.03
988	**-0.30**	**-0.44**	**-1.83**	0.06	0.04	0.20	0.13	0.09	0.39
995	-0.20	**-0.41**	**-3.93**	0.17	0.11	0.52	0.34	0.22	1.04

The reason for the rejection of H_0 when all antennas are tested together must depend on the differences between the antenna types or radome types (with and without). The difference of the means of the residual offsets between the antenna types in L2 up component is -5.3±0.4mm (Ashtech minus Leica). Also in North and East components there are clear difference, -0.2 and +0.7 mm, respectively. The test statistics show the same what we can see in Fig. 4.

Table 2. Test statistics

All antennas, the reference is the mean of the residual offsets off all antennas					
Test statistic/solution	L1	L2	Table $F_{u,r}$	H_0/L1	H_0/L2
$\frac{(O_X-0)^T C_X^{-1}(O_X-0)}{u_X} \sim F_{u_X,r}$	2.99	11.34	1.53	**rejected**	**rejected**
$\frac{(O_{ne}-0)^T C_{ne}^{-1}(O_{ne}-0)}{u_{ne}} \sim F_{u_{ne},r}$	3.19	7.34	1.61	**rejected**	**rejected**
$\frac{(O_{up}-0)^T C_{up}^{-1}(O_{up}-0)}{u_{up}} \sim F_{u_{up},r}$	2.59	19.52	1.80	**rejected**	**rejected**
Ashtech antennas, the reference is the mean of the residual offsets off Ashtech antennas					
Test statistic/solution	L1	L2	Table $F_{u,r}$	H_0/L1	H_0/L2
$\frac{(O_X-0)^T C_X^{-1}(O_X-0)}{u_X} \sim F_{u_X,r}$	0.91	2.82	1.69	accepted	**rejected**
$\frac{(O_{ne}-0)^T C_{ne}^{-1}(O_{ne}-0)}{u_{ne}} \sim F_{u_{ne},r}$	0.94	1.74	1.82	accepted	accepted
$\frac{(O_{up}-0)^T C_{up}^{-1}(O_{up}-0)}{u_{up}} \sim F_{u_{up},r}$	1.03	4.78	2.13	accepted	**rejected**
Leica antennas, the reference is the mean of the residual offsets off Leica antennas					
Test statistic/solution	L1	L2	Table $F_{u,r}$	H_0/L1	H_0/L2
$\frac{(O_X-0)^T C_X^{-1}(O_X-0)}{u_X} \sim F_{u_X,r}$	0.86	1.39	1.66	accepted	accepted
$\frac{(O_{ne}-0)^T C_{ne}^{-1}(O_{ne}-0)}{u_{ne}} \sim F_{u_{ne},r}$	0.77	1.47	1.77	accepted	accepted
$\frac{(O_{up}-0)^T C_{up}^{-1}(O_{up}-0)}{u_{up}} \sim F_{u_{up},r}$	1.03	1.22	2.06	accepted	accepted

6. CONCLUSIONS

We have found significant residual offsets in L2 Up components between two antenna types which we tested in Metsähovi in summer 2011. In our experiment we had same type of antenna platform in each pillar. Basically the pillars have similar construction but one of them in our test has different shape. There seems to be biases in the antenna calibration tables which propagate to the coordinates if we use the different antenna types in the same campaign. Since the antenna calibration is only valid for the near field that prevailed during calibration we may not rule out the conclusion that near-field effect would be a source of the difference. Because our tests indicate antenna or antenna type specific residual offsets and we can't isolate near-field effect from the results, we cannot claim that it would be the only reason for the residual offsets. We will continue our tests using different mountings in different location and environments.

We estimated offset values relative to the mean of all offsets or relative to one antenna. If we use the antennas which were in our test in the same campaign we can remove the offset biases between the antennas using the values estimated here but we cannot generalize the results to consider all the antennas of same type. The coordinate time series can have jumps due to the antenna change although individual absolute calibration values have been used. The size of the jump may be in cm level if also the type of the antenna has been changed.

Currently our recipe for the best precision is to minimize the possible near-field effects. This may be done by using similar antenna platforms of same height together with only one type of individually calibrated antennas.

REFERENCES

Bányai (2005): Investigation of GPS antenna mean phase center offsets using a full roving observation strategy. Journal of Geodesy 79:222-230. DOI 10.1007/s00190-005-0462-1.

Dach. R.. U. Hugentobler. P. Fridez and M. Meindl, 2007: Bernese GPS Software. Version 5.0. Astronomical Institute. University of Bern.

Görres et al., 2006: Absolute calibration of GPS antennas: laboratory results and comparison with field and robot techniques. GPS Solution (2006) 10: 136-145. DOI 10.1007/s10291-005-0015-3.

Kallio, U., Ahola, J., Koivula, H., Poutanen, M. (2009): GPS operations at Olkiluoto, Kivetty and Romuvaara in 2008. Working Report 2009-75. POSIVA Oy, Olkiluoto.

Koivula, H., P. Häkli, J. Jokela, A. Buga, R. Putrimas (2011): GPS metrology – bringing traceable scale to local crustal deformation network. In S. Kenyon et al. (eds.), Geodesy for Planet Earth, International Association of Geodesy Symposia 136, DOI 10.1007/978-3-642-20338-1_13, Springer-Verlag Berlin Heidelberg 2011. (in print)

Mader, G.L. (1999): GPS antenna calibration at the National Geodetic Survey. GPS Solutions, 3:50-58.

Wübbena, G., M. Schmitz, F. Menge, V. Böder, and G. Seeber (2000): Automated absolute field calibration of GPS antennas in real time. Proceedings of ION GPS 2000, 19-22 September, Salt Lake City, Utah, USA.

Zeimetz, P. and Kuhlmann H. (2011): Validation of the Laboratory Calibration of Geodetic Antennas based on GPS Measurements. International Federation of Surveyors Article of the Month – February 2011

BIOGRAPHICAL NOTES

Ulla Kallio, Hannu Koivula, Sonja Nyberg, Pasi Häkli, Paavo Rouhiainen and Veikko Saaranen work as research scientists in Finnish Geodetic Institute

Zane Cirule, Didzis Dobelis and Vladimirs Golovka visited Finnish Geodetic Institute in summer 2011 in ERASMUS program and at present are students in Riga Technical University

CONTACTS

Ulla Kallio
Finnish Geodetic Institute
Geodeetinrinne 2
P.O.Box 15
FI-02431 MASALA
FINLAND
Email: ulla.kallio@fgi.fi